JES Focus Issue on Mechano-Electro-Chemical Coupling in Energy Related Materials and Devices

Chemical Strain and Oxidation-Reduction Kinetics of Epitaxial Thin Films of Mixed Ionic-Electronic Conducting Oxides Determined by X-Ray Diffraction

R. Moreno,[a,b] J. Zapata,[a,b] J. Roqueta,[a,b] N. Bagués,[a,b] and J. Santiso[a,b,*,z]

[a]*Institut Catala de Nanociencia i Nanotecnologia (ICN2), Bellaterra, Barcelona 08193, Spain*
[b]*Consejo Superior de Investigaciones Científicas (CSIC), Bellaterra, Barcelona 08193, Spain*

X-ray diffraction, at high T's and switching between N_2/air atmospheres, was used to compare the chemical expansion due oxygen non-stoichiometry variations between epitaxial films of different mixed ionic-electronic conductors: $La_{0.6}Sr_{0.4}CoO_{3-\delta}$(LSC), $Ba_{0.5}Sr_{0.5}Co_{0.8}Fe_{0.2}O_{3-\delta}$(BSCF), $LaNiO_{3-\delta}$(LNO), $La_2NiO_{4+\delta}$(L2NO) and $GaBaCo_2O_{5.5+\delta}$(GBCO) and $La_{0.7}Sr_{0.3}MnO_{3-\delta}$(LSM). LSC and BSCF show the largest relative change in the cell parameter $\Delta c/c = +0.5\%$, while L2NO and GBCO show negative $\Delta c/c = -0.2\%$ and -0.1%, respectively. LNO and LSM show either reduced or negligible chemical expansions. In all cases the values correspond to their particular defect equilibrium and degree of charge localization. The oxygen surface exchange kinetics was also evaluated from in-situ time-resolved analyses of the cell parameter variations. LSC, LNO and GBCO films show fast oxygen reduction kinetics, $k_{chem} = 5 \cdot 10^{-6}$, $3 \cdot 10^{-6}$, and $2 \cdot 10^{-7}$ cm/s at 700°C, respectively, in relative agreement with reported values, while BSCF films show much slower kinetics than expected, below $k_{chem} = 10^{-7}$ cm/s at 650°C, related to the degradation process observed in the films.
 [DOI: 10.1149/2.0091411jes]

Manuscript submitted June 20, 2014; revised manuscript received August 27, 2014. Published September 4, 2014. This was Paper 360 presented at the Orlando, Florida, Meeting of the Society, May 11–15, 2014. *This paper is part of the JES Focus Issue on Mechano-Electro-Chemical Coupling in Energy Related Materials and Devices.*

The study of the chemical strain in transition metal oxides induced by the oxygen non-stoichiometry changes upon oxygen surface exchange with the atmosphere, as well as its particular kinetics at elevated temperatures, is of increasing relevance for understanding the fundamental mechanisms for oxygen reduction and evolution reactions (ORR/OER) of oxide catalysts,[1] as well as for novel cathode materials for intermediate-temperature solid oxide fuel cell (SOFC) technology.[2] In this work we determine the chemical strain and kinetics of a collection of mixed ionic-electronic conducting (MIEC) oxide materials in the perovskite family ABO_3 (A = La, Sr, Ba, Gd) and (B = Ni, Co, Mn) typically used as cathodes in intermediate-temperature solid oxide fuel cells. We compare the results obtained by time-resolved X-ray diffraction with those in literature obtained with other techniques in order to further validate this technique and to determine the performance of these compounds into electrochemical devices.

Depending on the type of material, temperature and oxygen partial pressure conditions the surface exchange reactions may involve different defects. Typically, for oxygen deficient perovskite materials at high pO_2 the dominant point defects are oxygen vacancies, $V_O^{\bullet\bullet}$ (in Kröger-Vink notation) and electron holes, $h^\bullet$, and, therefore, oxygen incorporation from the atmosphere into the solid follows the reaction:

$$\tfrac{1}{2}O_2^{gas} + V_O^{\bullet\bullet} \leftrightarrow O_O^X + 2h^\bullet \quad [1]$$

where the oxygen gas molecule is adsorbed on the surface, dissociates an incorporates into the oxygen vacancies in the solid generating electron holes (in this case of a p-type material). However, in other materials or different conditions the dominant oxide defects might be Oxygen interstitials O_i'', and the oxygen incorporation reaction takes the form

$$\tfrac{1}{2}O_2^{gas} \leftrightarrow O_i'' + 2h^\bullet \quad [2]$$

In both cases, the electronic charges might be localized in the transition metal ions that are oxidized (for instance, $M^{3+} \rightarrow M^{4+}$, in a case of M^{3+} being the equilibrium ground state)

$$\left[M_M^{3+}\right]^\times + h^\bullet \leftrightarrow \left[M_M^{4+}\right]^\bullet \quad [3]$$

These reactions, along with other reactions involving the point defects in the solid and the condition for charge neutrality, establish in each case the particular defect equilibrium which relate the concentration of all point defect species, including the oxygen non-stoichiometry, at a given pO_2 and T.[3] In addition, in Co-oxides, as well as in Mn oxides, it is generally accepted that charge disproportionation occurs between different valence states of the metal ion following

$$2[M^{3+}]^\times \leftrightarrow [M^{2+}]' + [M^{4+}]^\bullet \quad [4]$$

Taking into account the mass action laws for the different reactions, along with charge neutrality conditions, a power dependency of the non-stoichiometry with the oxygen partial pressure is generally obtained $\delta \propto {pO_2}^{-m}$, and so it is for the oxygen surface exchange kinetics $k \propto {pO_2}^{-m}$, where the exponent accounts for the defect chemistry of the material along with the rate-determining step in the overall oxygen incorporation reaction, ranging from 0.5 to 1.0 values.[1,2,4,5]

In most transition metal oxide materials the variation in the oxygen non-stoichiometry δ produced by oxygen exchange with the atmosphere is often accompanied by subtle cell volume changes, the so-called chemical strain. Generally, the incorporation of oxygen point defects (oxygen vacancies or interstitials) is expected to cause a cell expansion from the equilibrium intrinsic cell. In most cases this expansion depends on the variations in the radii of the transition metal ions with variable oxidation state. Although, other factors have to be taken into account, like the degree of charge localization, the effective radii of the associated oxygen defects, the Coulomb repulsion between those defects, as well as other structure features in more complex layered structures.[6] In this way any slight variation in the oxygen content would correspondingly result in a measurable cell volume increase. The ability to dynamically follow the cell volume variations allows establishing a direct correlation with oxidation/reduction kinetics.

X-ray diffraction is a powerful technique to determine subtle changes in the cell parameters of crystalline materials. Recently,

*Electrochemical Society Active Member.
zE-mail: jsantiso@cin2.es

it has been demonstrated in epitaxial thin films that conventional X-ray diffractometers may be used to determine average cell parameter changes as small as 0.1 ppm in redox cycles with time resolution of only a few seconds, which have been used to analyse the oxygen surface exchange kinetics of $La_2NiO_{4+\delta}$ compound.[7] This technique has the advantage of being contactless and allows a selective detection of one particular phase in thin film heterostructures, thus avoiding convolution with possible substrate effects.

Experimental

Epitaxial films with thickness of about 40 to 80 nm have been obtained by Pulsed Laser Deposition from stoichiometric dense ceramic targets of $LaNiO_{3-\delta}$ (LNO), $La_{0.6}Sr_{0.4}CoO_{3-\delta}$ (LSC), $Ba_{0.5}Sr_{0.5}Co_{0.8}Fe_{0.2}O_{3-\delta}$ (BSCF), $La_{0.7}Sr_{0.3}MnO_{3-\delta}$ (LSM) compounds with perovskite structure, as well as perovskite-related $La_2NiO_{4+\delta}$, (L2NO) and $GdBaCo_2O_{5.5+\delta}$ (GBCO) compound. For GBCO we used Co-enriched targets to compensate for the observed cation composition deviations (Co-deficiency) in the deposited films.[8] All films were deposited on $SrTiO_3$ (001) single crystal substrates (STO, 5 × 5 mm^2, 0.5 mm thick, from Crystec GmbH) at deposition temperatures from 600 to 800°C, and oxygen pressures from 100–300 mTorr, which enable the epitaxial growth due to the close matching of film and substrate structures. Under these conditions the films of the referred materials grow with the *c*-axis orientation. Generally the films are very smooth (surface roughness below 1 nm). In some cases such as in LSMO/STO they even show single unit-cell (0.39 nm) stepped terraces. Other materials, like BSCF are prone to form CoO_x outgrowths, which increase the overall film roughness. The films do not show columnar structures (no apparent vertical domain walls observed) unless the thickness grows above 200–500 nm, depending on the material. Film thickness variations are less than about ±5% in the area of the samples used in the present experiments.

X-ray diffraction reciprocal space maps of different asymmetric H0L reflections were measured for the as grown films. For each compound a proper selection of the most suitable reflections was made, in the area close to the −103 STO reflection, in order to obtain a good compromise between high XRD intensity and adequate geometry for the time-resolved experiments, as described in detail in a previous study.[7] These reflections correspond to the equivalent −103 reflection for primitive perovskite structure (LSC, BSCF, LNO, LSM), and −106 and −1–110 for the GBCO and L2NO layered compounds, respectively.

The samples were placed in a XRD domed hot stage (Anton Paar, DHS1100, internal volume 52 cm^3, plus 19 cm^3 gas tubing) and exposed to air/N_2 atmosphere cycles (1000 sccm gas flows) at different temperatures from 450 to 700°C (gas flushing time <3 sec). XRD fast static scans of asymmetric H0L reflections were collected, at time intervals of about 10 sec duration (minimum acquisition time for 256-channel PIXcel X-ray solid-state linear detector is 2 sec) The time between gas changes was varied between 2 to 4 hours in order to achieve almost full stabilization of the corresponding film oxygen stoichiometry. The out-of-plane parameter of the film material was calculated from the measured scans. The conditions for the acquisition were the same as those previously described in Ref. 7.

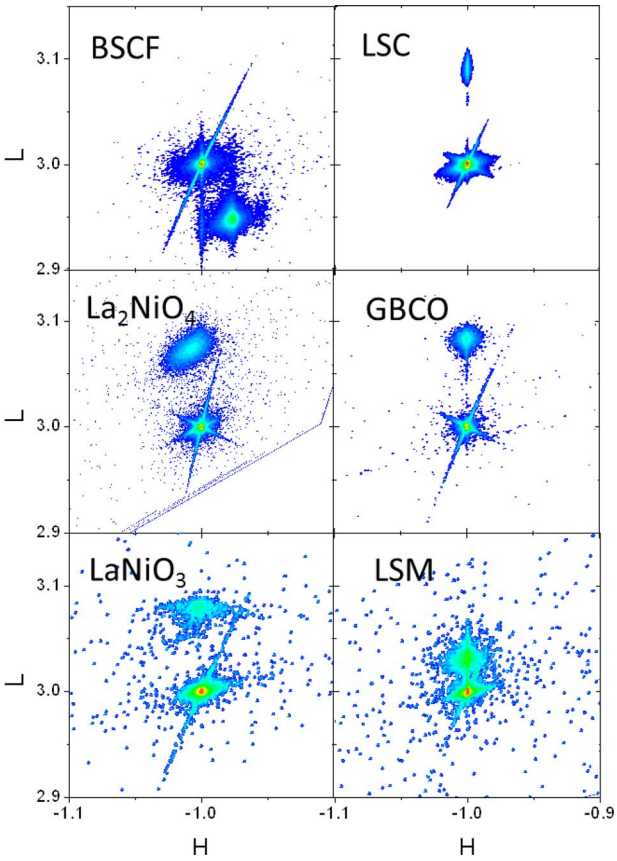

Figure 1. XRD Reciprocal space maps of the chosen reflections for the different materials.

Results and Discussion

Fig. 1 shows X-ray diffraction reciprocal space maps of the reflections that were used for the cell parameter determination. The most intense reflection at H = −1, L = 3 corresponds to −103 STO reflection, except for La_2NiO_4 on STO where we chose the reflection close to −1 −1 3 STO. For LSC, GBCO, $LaNiO_3$ and LSM film and substrate reflections show perfect alignment in the vertical direction, which indicates full matching with in-plane substrate cell parameter. However, BSCF and $La_2NiO_{4+\delta}$ films show H position different to the STO, which correspond to almost fully relaxed films. The choice of HKL reflections for the different materials is also reflected in Table I, which contains as well the out-of-plane cell parameters measured at room temperature for the different materials. All the film materials, except for BSCF, show L value larger than the STO substrate, which corresponds to out-of-plane parameters shorter than the STO ($a = 3.905$ Å).

Oxygen stoichiometry expansion.— Figure 2 shows the out-of-plane cell parameter variations obtained for the different compounds

Table I. Different compounds deposited in the form of epitaxial thin films.

Compound	Film thickness	Out-of-plane cell parameters	Chosen HKL reflection
$La_{0.6}Sr_{0.4}CoO_{3-\delta}$ (LSC)	50 nm	$c = 3.790$ Å (±0.0002 Å)	−103
$Ba_{0.5}Sr_{0.5}Co_{0.8}Fe_{0.2}O_{3-\delta}$ (BSCF)	80 nm	$c = 3.980$ Å	−103
$LaNiO_{3-\delta}$	44 nm	$c = 3.859$ Å	−103
$La_{0.67}Sr_{0.33}MnO_3$ (LSM)	40 nm	$c = 3.880$ Å	−103
$La_2NiO_{4+\delta}$	50 nm	$c = 12.641$ Å	−1–1 10
$GdBaCo_2O_{5.5+\delta}$ (GBCO)	51 nm	$c/2 = 3.895$ Å	−106
$SrTiO_3$ (substrate)		$c = 3.905$ Å	−103

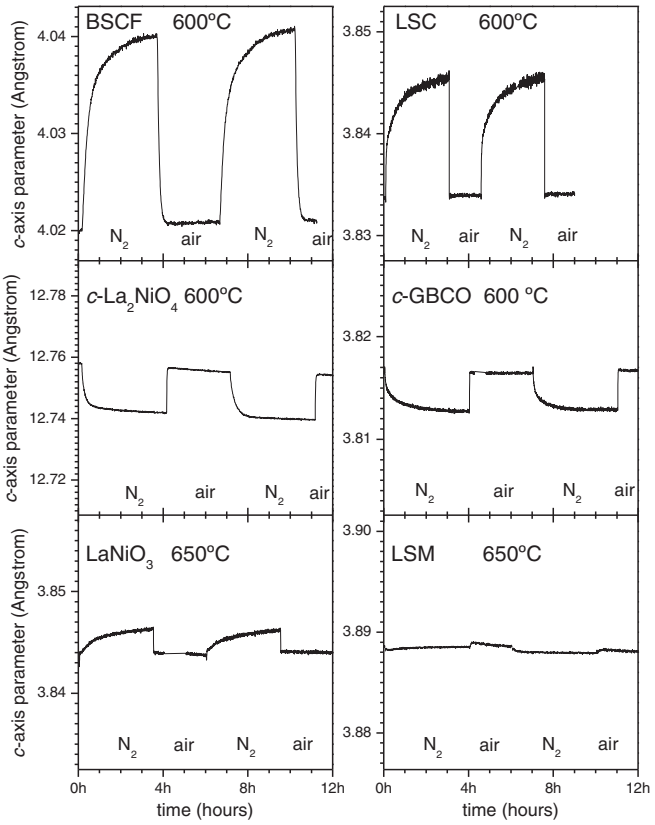

Figure 2. Variation of the out-of-plane cell parameter of BSCF, LSC, L2NO, GBCO, LNO and LSM films of about 40 nm thickness deposited on $SrTiO_3$(100) substrates, as measured by XRD at temperatures of about 600–650°C and air/N_2 atmosphere cycling.

upon air/N_2 cycling at temperatures around 600°C. The error in the cell parameters determination was below 0.0002 Å. Similar curves were acquired at different temperatures in order to obtain information about the temperature dependency. The average cell parameters increase upon increasing temperature as results of thermal expansion. At a given temperature the cell parameters vary under N_2 or air atmosphere depending on the chemical strain associated to the changes in their oxygen stoichiometry.

As it is observed the out-of-plane cell parameter for BSCF, around $c = 4.02$ Å (in air at 600°C) is substantially larger than for the rest of perovskite compounds LSC, LNO, LSMO where the c-axis is always below $c = 3.9$ Å. This is related to the large size of the Ba^{2+} ion compared to La^{2+} and Sr^{3+}. For c-axis oriented GBCO the out-of-plane parameter in the graph corresponds to $c/2$ (cell is doubled along c-axis because of Gd/Ba alternate sequence). For La_2NiO_4 c-axis parameter is not related to perovskite because it is a Ruddelsden-Popper layered structure. The vertical axis in the graphs has been scaled to show the same relative changes, therefore the magnitude of the observed changes between N_2 and air atmosphere offers a direct comparison of the chemical strain magnitude for the different compounds.

The first remarkable difference is the sign of the cell parameter change. For $La_{0.6}Sr_{0.4}CoO_{3-\delta}$, $Ba_{0.5}Sr_{0.5}Co_{0.8}Fe_{0.2}O_{3-\delta}$ and $LaNiO_{3-\delta}$ the out-of-plane parameter shows a larger value under N_2 atmosphere than in air atmosphere. Conversely, $La_2NiO_{4+\delta}$ and c-axis oriented GBCO show larger out-of-plane cell parameter in air than in N_2. LSM does not significantly change its parameter under air/N_2 cycling.

In epitaxial thin films (thickness below 100 nm) the in-plane cell parameters are not expected to vary substantially when changing the atmosphere, because of the matching with the substrate structure inhibiting the in-plane expansion or contraction. Even in fully relaxed

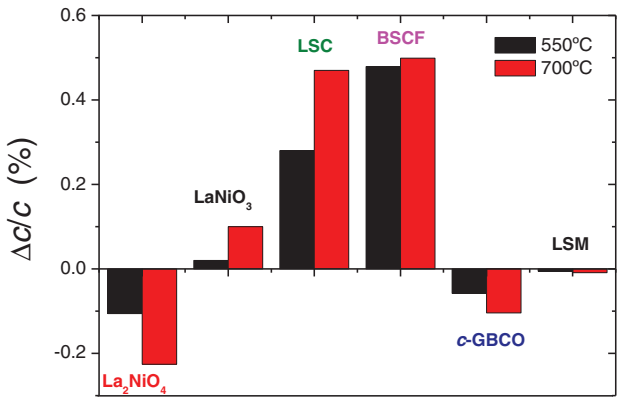

Figure 3. Relative variation of the out-of-plane cell parameters for the collection of analysed compounds: L2NO, LNO, LSC, BSCF, GBCO and LSM, measured at two different temperatures 550 and 700°C.

films, like BSCF, it was not observed any substantial variation of the in-plane parameter between N_2 and air atmospheres. In BSCF/STO a large compressive stress should develop under N_2 atmosphere, because of the increase of the equilibrium cell volume. Therefore, relaxation would result in a progressive reduction of the c-axis expansion, which was never observed. This indicates that no significant misfit strain relaxation occurs in the films in the temperature range and at the timescale of the exchange measurements. Consequently, it is expected that the stress associated with the stoichiometry changes in the in-plane direction, either compressive (BSCF) or tensile (LSC), is fully transformed into an elastic response of the out-of-plane direction causing an additional strain. Hence, the extent of the out-of-plane parameter differences may be directly related, in a first approximation, to that of the bulk material overall cell volume chemical expansion.

For a clearer comparison between the materials, and given the uncertainties in the reported defect equilibrium, we have considered more sensible to present the direct experimental differences between out-of-plane cell parameters in air and N_2 as a comparison of their chemical expansion coefficients, rather than trying to calculate a correlation between structural changes and the corresponding δ values, which will be subject of a further study.

Assuming this criteria, Fig. 3 depicts the values of the relative difference in the cell parameters $(c_{N2} - c_{air})/c_{N2}$ at two temperatures, 550 and 700°C, for the compounds grown as thin epitaxial films on $SrTiO_3$(100) single crystal substrates. The positive cell volume change observed in LNO, LSC and BSCF, upon increasing the oxygen vacancies concentration, corresponds to the expected behavior for oxygen deficient perovskites.[9] In our measurements, LSC and BSCF show the largest expansions of the order of 0.5% at 700°C. This is in agreement with the general idea that Co-containing oxides present the largest values for the chemical expansion coefficient among the peroskites.[10] In $La_{0.8}Sr_{0.2}CoO_{3-\delta}$ epitaxial films a reversible expansion of about +0.9% has been reported after long exposure to severe reducing conditions (2% CO in He at 550°C) with respect to pure O_2.[11] This is probably the limit between fully oxidized and fully reduced $La_{0.8}Sr_{0.2}CoO_{3-\delta}$ material. The pO_2 atmosphere differences between N_2 and air used in our experiment are still far from these values, and therefore, less subject to possible non-linear effects due to oxygen vacancy concentration saturation. It is interesting to point out that in the same study similar values of oxygen non-stoichiometry were attained by applying a negative bias of −0.6 V in a Pt/LSCO/YSZ/Pt electrochemical cell configuration. A previous report in $La_{0.6}Sr_{0.4}CoO_3$ bulk material has shown a variation in the chemical expansion measured by dilatometry of about +0.5% when varying the non-stoichiometry content from $\delta = 0.06$ to 0.14 in $pO_2 = 0.21$ atm and 10^{-5} atm, respectively, at about 700°C.[12] This value of expansion coincides with that measured in the present experiment.

The chemical expansion value of +0.5%, obtained for BSCF material both at 550 and 700°C, is substantially higher than those extracted from reported cell parameters increase of about +0.17% and +0.24%, at 600 and 700°C respectively, measured by neutron diffraction in BSCF ceramic pellets exposed to 1 and 10^{-3} atm O_2.[13] It is very likely that this difference is related to the epitaxial nature of the present films. While in bulk polycrystalline material the cell expansion takes place uniformly along the three dimensions of the crystal domains, the epitaxial films concentrate the expansion along out-of-plane axis, and therefore may show about 3-fold larger expansion. A comparison of the full cell volume expansion would then render comparable values with reported bulk material. However, it is not ruled out that the discrepancy values might be related to a slight difference in the cation composition in such complex material, which is prone to segregation and to degradation by phase transformation,

For LNO films a value of +0.1% is observed at 700°C. Even in high pO_2 Ni^{3+} is unstable and reduces to Ni^{2+}. Therefore, important non-stoichiometry is expected for $LaNiO_{3-\delta}$ compound. In fact it is known to decompose in air at moderate temperatures about 900°C.[14] Epitaxial growth may prevent decomposition and reversible redox cycles have been performed in the present films. Oxygen ordered $La_2Ni_2O_5$, a reduced form of $LaNiO_{2.5}$ phase, is reported to have considerable larger cell volume 57.03 Å^3,[15] compared with stoichiometric $LaNiO_3$ rhombohedral phase (cell volume = 56.58 Å^3).[16] This represents an increase of about +0.8%. The observed chemical expansion of about +0.1% at 700°C indicates that either the epitaxial growth prevents the film for a large oxygen composition variation, or the metallic character of the material with highly delocalized electronic charge reduces the chemical expansion despite the oxygen stoichiometry changes. This remains still unclear and needs further investigation.

A negative value of $\Delta(c_{N2} - c_{air})/c = -0.2\%$ at 700°C was measured for $La_2NiO_{4+\delta}$. This corresponds to an expansion when increasing the oxygen content, which is characteristic of the incorporation of oxygen interstitials. The same value was already reported along the *c*-axis of $La_2NiO_{4+\delta}$ bulk ceramic samples ($\Delta c/c = -0.2\%$, from $pO_2 = 10^{-5}$ to 0.21 atm and 700°C).[17] However, in bulk ceramic $La_2NiO_{4+\delta}$ the *a,b*-cell parameters respond with opposite sign to the oxygen stoichiometry changes ($\Delta a/a = +0.05\%$), so the overall cell volume expansion becomes compensated and the volume change becomes very small ($\Delta V/V = -0.1\%$). The observation in the present films of $\Delta c/c = -0.2\%$ at 700°C, with no significant in-plane expansion, is an indication that in epitaxial films the overall expansion might be dominated, at least in this layered compound, by that of *c*-axis expansion. Very little effect is produced due to the change in ionic radii of Ni as reported to be the main responsible for strain along the *a,b* plane in bulk material.[13] Therefore, the major effect is produced by the variation in the concentration of interstitial oxygen in the La-O rock salt layers of the structure and their Coulomb repulsion.

A similar situation occurs in *c*-axis oriented GBCO material. We measured negative $\Delta c/c = -0.1\%$ at 700°C, which suggests a dominant effect of oxygen interstitials. However, in this compound the real nature of the oxygen defects remains still unclear.[18]

Contrary to the significant response of previously described oxides, LSM films did not show any substantial chemical strain. Sr-substituted $LaMnO_3$ presents very low concentration of oxygen vacancies in the pO_2 region between 10^{-5} to 1 atm, and more severe reducing conditions (lower pO_2, higher *T*) are needed to produce a certain oxygen nonstoichiometry.[19] Under those conditions a substantial chemical expansion is expected as reported in $LaMnO_{3-\delta}$ compound.[20,21]

Surface oxygen exchange kinetics.— XRD time-resolved cell parameter variations, like those shown in Fig. 2 for the different compounds, allowed determining oxidation/reduction time responses, which are directly related to the oxygen surface exchange kinetics. For a given temperature, as it was shown in Fig. 2 around 600°C, the cell parameters after changing the gas atmosphere reached full stabilization for the oxidation from N_2 to air for all compounds (which shows an step like change in the time scale depicted in the graphs), while it is not fully stabilized during the reduction step from air to N_2, given the slower kinetics of this process. In this work we concentrate into the oxidation kinetics, which is related to the Oxygen reduction reaction, while film reduction would be related to the Oxygen evolution reaction. Fig. 4 depicts an expanded view of the time response of the cell parameter variation during the first N_2 to air oxidation step of Fig. 2 for the different materials at 600°C (650°C for L2NO and LSM). The graph also includes the fit for a single exponential dependency. Note that for LSC material despite the fast exchange rate, that reaches almost saturation in the first measured point, it is still possible to estimate a response time ($\tau = 3.8 \pm 1.5$ sec). BSCF presents a very slow exchange rate that does not reach fully stabilization in the time span of the graph. LSM does not show any significant chemical expansion.

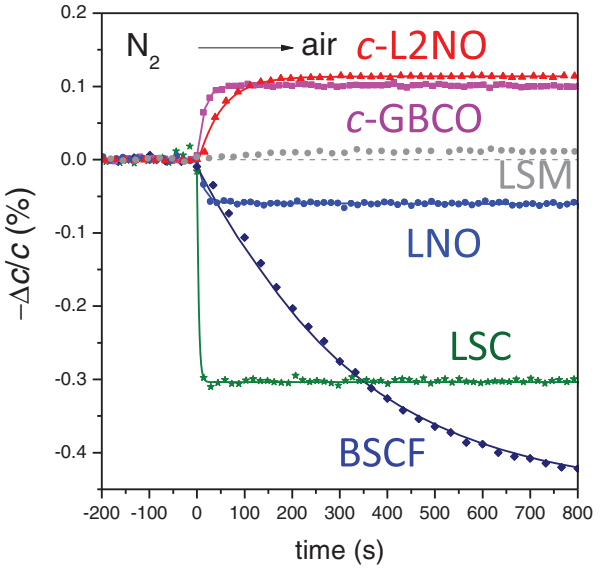

Figure 4. Time dependency of the out-of-plane cell parameters for the different materials in the first N_2 to air oxidation step. The continuous line corresponds to the single exponential fit.

In most of the analysed compounds, the time dependency for either oxidation or reduction is described with an exponential function with a single time response, τ. Oxygen surface exchange rate is, then, calculated as $k_{chem} = d/\tau$, where *d* is the thickness of the film, assuming a negligible contribution of oxygen diffusion due to their small thickness. For some heterostructures, like $La_2NiO_{4+\delta}$ on $SrTiO_3$, the time dependency is better described in terms of "fast" and "slow" exponential components, with two different characteristic time responses, τ_1 and τ_2, as described in a previous work,[7] being the "slow" response related to a possible oxygen exchange with the substrate. Despite this fact, and in order to facilitate the comparison between materials, a single characteristic time response, τ*, is used in all cases, being τ* the time necessary to reach 0.63 (=1/e) of the total normalized change from air to N_2 at a given temperature (note that $\tau = \tau^*$ for single exponential).

Some of the results for the oxidation kinetics of the different cathode materials are depicted in Fig. 5.

As it is clearly depicted in the figure the fastest oxidation kinetics, corresponding to the oxygen reduction reaction at the surface, has been obtained for $La_{0.6}Sr_{0.4}CoO_3$ (LSC) material. At 700°C we obtained values of $k_{chem} = 5(\pm 3) \cdot 10^{-6}$ cm/s. These values extrapolate to comparable values at higher temperatures reported in literature for LSC thin films: $k = 10^{-4}$-10^{-5} cm/s for $La_{0.6}Sr_{0.4}CoO_3$ films ($pO_2 = 10^{-2}$ bar @825°C);[22] $4 \cdot 10^{-6}$ cm/s in $La_{0.8}Sr_{0.2}CoO_3$ films (pO_2 = 1atm @520°C);[23] or $2 \cdot 10^{-6}$ cm/s for $La_{0.5}Sr_{0.5}CoO_3$ films (pO_2 = 1atm @700°C).[24] And these values are larger than those reported in $k = 5.4 \cdot 10^{-7}$ cm/s for $La_{0.6}Sr_{0.4}CoO_3$ PLD films ($pO_2 = 10^{-1}$ bar @700°C);[25] but are considerable lower than $k = 10^{-4}$-10^{-5} cm/s reported for $La_{0.8}Sr_{0.2}CoO_3$ (pO_2 = 1atm and temperatures as low

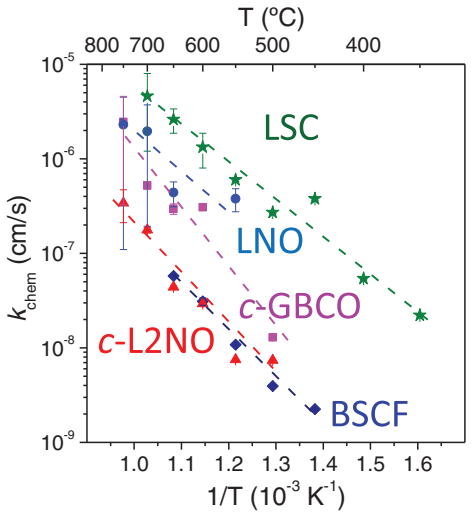

Figure 5. Arrhenius plot of the oxidation kinetics of the different epitaxial films obtained from the cell parameter variations when the gas atmosphere changes from N_2 to air. (Error bars are only visible when being larger than the symbol size)

as 520°C).[26] The increase in surface exchange coefficient in this last work, and subsequent reports from the same group and collaborators, was attributed to the presence of a Ruddlesden-Popper related phase $La_{2-x}Sr_xCoO_4$ phase ("214") at the surface that exerts a catalytic effect for the Oxygen chemisorption and dissociation.[26,27] Activation energy of k was calculated to be of about $E_a = 0.77$ (±0.1) eV among the lowest values reported in literature from 0.5 to 1.2 eV.

$LaNiO_{3-\delta}$ (LNO) also showed fast oxidation kinetics, between $k = 3 \cdot 10^{-6}$ at 700°C, comparable to that of LSC. That was already predicted by the similar occupancy close to unity of the corresponding $3d$ e_g levels of the transition metal ions, which is believed to determine the oxygen reduction and evolution reactivity of transition metal oxides.[28] However, the small chemical expansion of less than 0.1% change in the cell parameters for $LaNiO_3$, did not allow extracting reliable values in the low temperature range below 500°C. This low chemical expansion is probably related to the high metallic character of this compound and important charge delocalization.[10]

C-axis oriented films of the layered compounds $GdBaCo_2O_{5.5+\delta}$ and $La_2NiO_{4+\delta}$ films showed k values in excess of 10^{-6} cm/s and about $4 \cdot 10^{-7}$ cm/s, respectively, at 700°C, with larger activation energies than that of LSC (as observed by the larger slopes in the Arrhenius plot), which considerably reduce their oxidation kinetics in the low temperature region. Their respective activations energies are E_a = 1.32 and 1.11 eV, much larger than those reported in thin epitaxial films with the same c-axis orientation measured by IEDP-SIMS of 0.60 eV[8] and 0.38eV,[29] respectively.

The most intriguing results correspond to $Ba_{0.5}Sr_{0.5}Co_{0.8}Fe_{0.2}O_{3-\delta}$ (BSCF), which despite of being considered one of the most active materials for oxygen reduction,[28] k values obtained for the thin films in this work are considerable lower than for LSC material, below $k = 10^{-7}$ cm/s at 650°C, and lower than those measured by EIS on BSCF microelectrodes of about $k = 8 \cdot 10^{-6}$ cm/s (pO_2 = 1atm O_2 at 700°C)[2] and by conductivity relaxation $k = 6 \cdot 10^{-4}$ cm/s (pO_2 = 1atm O_2 at 700°C).[30] Activation energy of k was calculated to be of about $E_a = 0.98$ eV, much lower than that previously reported of $E_a = 1.6$ eV.[2] The reduced k values are probably related to a large degradation of the surface hindering the oxygen adsorption and dissociation. This behavior contrasts with the large values of the chemical expansion of about 0.5% depicted in Fig. 3, which may be an indication that the main source of degradation takes place at the surface of the material. Although, it cannot be ruled out that additional degradation within the volume of the films is also occurring, as observed by the progressive reduction of the XRD signal upon successive cycling (shown in supplementary information). Despite the measured k values for LSC are surprisingly in good agreement with literature, it is not discarded that the important pO_2 dependency of k reported for BSCF material ($m = 0.73$)[2] may reduce the effective k_{chem} values measured in our experiment (because of the large pO_2 change from N_2 to air) in a much larger extent for BSCF than for LSC ($m = 0.43$ at 675°C[31] and m = 0.37 at 725°C).[15]

Conclusions

Time-resolved X-ray Diffraction has been used to explore the cell structure expansion and compression upon changing the oxygen non-stoichiometry in epitaxial thin films of some typical transition metal oxides used as cathodes for intermediate-temperature SOFCs. The span of the cell structure variations after exposure of the films to air or N_2 atmospheres relates to their predominant oxygen defects, either oxygen vacancies or interstitials, and their magnitudes are in agreement with similar data reported in literature for LSC ($\Delta c/c \sim +0.5\%$), but much larger than reported for BSCF (+0.5%) and L2NO (−0.2%).

Oxygen surface exchange kinetics of the films have revealed large catalytic effect for the oxygen reduction on LSC in the whole range of temperatures analysed (from 400 to 700°C) with values comparable to a large group of studies in literature. C-axis oriented $LaNiO_3$ and GBCO films have also revealed a high k rate in the high temperature range around 700°C. On the other side BSCF films have revealed much lower activity for oxygen reduction than that reported in literature probably because of the combined effect of degradation, as well as an effect derived from the measurement technique, due to the large pO_2 dependency of k. Further studies reducing the pO_2 span to around one order of magnitude need to be conducted in order to establish a comparison with literature data. Nevertheless, it is widely demonstrated that the large number of factors affecting oxygen surface exchange kinetics in thin films makes difficult the comparison between experiments, being the reason for such a large spread in reported k values and activation energies in literature.

Acknowledgments

The authors acknowledge the Spanish Ministry of Education and Culture for financial support (MAT2011-29081-C02-01 and CONSOLIDER-INGENIO CSD2008-0023 projects). R. M. and J. R. thank the Spanish Ministry of Education for a FPI grant and PTA contracts.

References

1. S. B. Adler, X. Y. Chen, and J. R. Wilson, *J. Catal.*, **245**, 91 (2007).
2. L. Wang, R. Merkle, and J. Maier, *J. Electrochem. Soc.*, **157**, B1802 (2010).
3. S. R. Bishop, H. L. Tuller, Y. Kuru, and B. Yildiz, *J. Eur. Ceram. Soc.*, **31**, 2351 (2011).
4. L. Wang, R. Merkle, Y. A. Mastrikov, E. A. Kotomin, and J. Maier, *J. Mater. Res.* **27**, 2000 (2012).
5. M. H. R. Lankhorst, *J. Electrochem. Soc.*, **144**, 1268 (1997).
6. D. Marrocchelli, S. R. Bishop, H. L. Tuller, and B. Yildiz, *Adv. Funct. Mater.*, **22**, 1958 (2012).
7. R. Moreno, P. García, J. Zapata, J. Roqueta, J. Chaigneau, and J. Santiso, *Chem. Mater.*, **25**, 3640 (2013).
8. J. Zapata, M. Burriel, P. Garcia, J. A. Kilner, and J. Santiso, *J. Mater. Chem. A*, **1**, 7408 (2013).
9. M. H. R. Lankhorst, H. J. M. Bouwmeester, and H. Verweij, *J. Solid State Chem.*, **133**, 555 (1997).
10. S. R. Bishop, D. Marrocchelli, C. Chatzichristodoulou, N. H. Perry, M. B. Mogensen, H. L. Tuller, and E. D. Wachsman, *Annu. Rev. Mater. Res.* **44**, 205 (2014).
11. M. D. Biegalski, E. Crumlin, A. Belianinov, E. Mutoro, Y. Shao-Horn, and S. V. Kalinin, *Appl. Phys. Lett.*, **104**, 161910 (2014).
12. X. Chen, J. Yu, and S. B. Adler, *Chem. Mater.*, **17**, 4537 (2005).
13. S. McIntosh, J. F. Vente, W. G. Haije, D. H. A. Blank, and H. J. M. Bouwmeester, *Chem. Mater.*, **18**, 2187 (2006).
14. T. Nakamura, G. Petzow, and L. J. Gauckler, *Mater. Res. Bull.*, **14**, 649 (1979).
15. H. Falcon, A. E. Goeta, G. Punte, and R. E. Carbonio, *J. Solid State Chem.* **133**. 379 (1997).
16. J. A. Alonso, M. J. Martinez Lope, J. L. Garcia Munoz, and M. T. Fernandez, *Physica B, Condensed Matter* **234**, 18 (1997).

17. V. V Kharton, A. V. Kovalevsky, M. Avdeev, E. V. Tsipis, M. V. Patrakeev, A. A. Yaremchenko, E. N. Naumovich, and J. R. Frade, *Chem. Mater.*, **19**, 2027 (2007).
18. D. S. Tsvetkov, V. V. Sereda, and A. Y. Zuev, *Solid State Ionics* **180**, 1620 (2010).
19. J. Mizusaki, N. Mori, H. Takai, Y. Yonemura, H. Minamiue, H. Tagawa, M. Dokiya, H. Inaba, K. Naraya, T. Sasamoto, and T. Hashimoto, *Solid State Ionics*, **129**, 163 (2000).
20. A. Y. Zuev and D. S. Tsvetkov, *Solid State Ionics*, **181**, 557 (2010).
21. S. Miyoshi, J.-O. Hong, K. Yashiro, A. Kaimai, Y. Nigara, K. Kawamura, T. Kawada, and J. Mizusaki, *Solid State Ionics* **3–4**, 209 (2003).
22. W. Preis, E. Bucher, and W. Sitte, *J. Power Sources*, **106**, 116 (2002).
23. L. M. van der Haar, M. W. den Otter, M. Morskate, H. J. M. Bouwmeester, and H. Verweij, *J. Electrochem. Soc.*, **149**, J41 (2002).
24. X. Chen, *Solid State Ionics*, **146**, 405 (2002).
25. M. Sϕgaard, P. Vang Hendriksen, and M. Mogensen, *J. Solid State Chem.*, **180**, 1489 (2007).
26. G. J. la O', S. J. Ahn, E. Crumlin, Y. Orikasa, M. D. Biegalski, H. M. Christen, and Y. Shao-Horn, *Angew. Chemie Int. Ed.*, **49**, 5344 (2010).
27. E. J. Crumlin, E. Mutoro, S. J. Ahn, G. J. la O', D. N. Leonard, A. Borisevich, M. D. Biegalski, H. M. Christen, and Y. Shao-Horn, *J. Phys. Chem. Lett.*, **1**, 3149 (2010).
28. J. Suntivich, K. J. May, H. A. Gasteiger, J. B. Goodenough, and Y. Shao-Horn, *Science*, **334**, 1383 (2011).
29. M. Burriel, G. Garcia, J. Santiso, J. A. Kilner, R. J. Chater, and S. J. Skinner, *J. Mater. Chem.*, **18**, 416 (2008).
30. M. Burriel, C. Niedrig, W. Menesklou, S. F. Wagner, J. Santiso, and E. Ivers-Tiffée, *Solid State Ionics*, **181**, 602 (2010).
31. M. Mosleh, M. Sϕgaard, and P. V. Hendriksen, *J. Electrochem. Soc.*, **156**, B441 (2009).